Application of EUV Diffraction Optics for Actinic Mask Inspection and Metrology

Kenneth C. Johnson, KJ Innovation (kjinnovation@earthlink.net)
2018 EUVL Workshop P36 (euvlitho.com)

Actinic, Spot-Scanning EUV Microscope: Schematic Concept

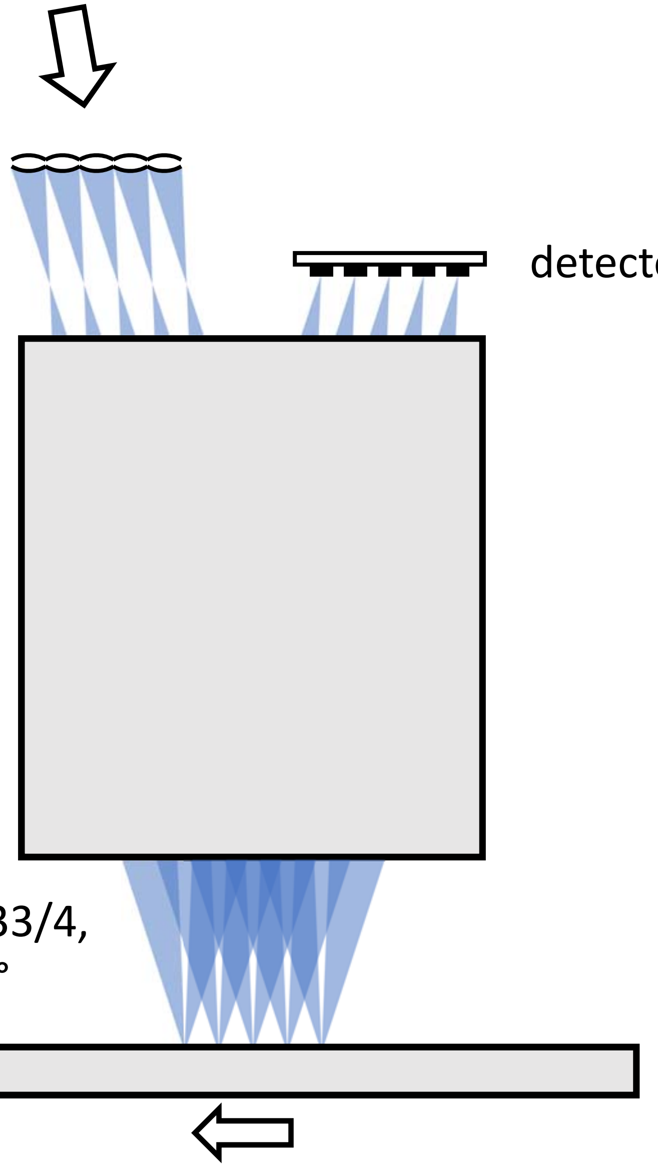

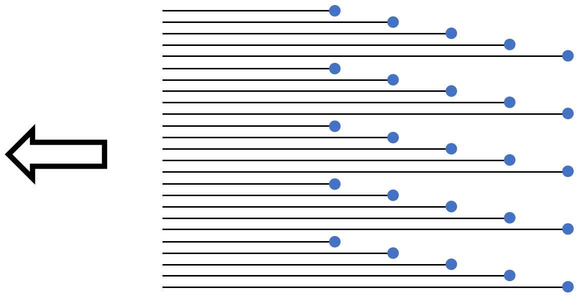

Presentation Outline

1. EUV microlenses can be fully achromatized over a 2% EUV spectrum.

2. Zero-aberration imaging can be achieved over a large image field with an ***economical*** projection system.

3. A parallel spot-scanning system could provide useful capabilities and benefits for actinic EUV inspection and metrology.

A Schupmann doublet lens is achromatic over the 2% EUV band.

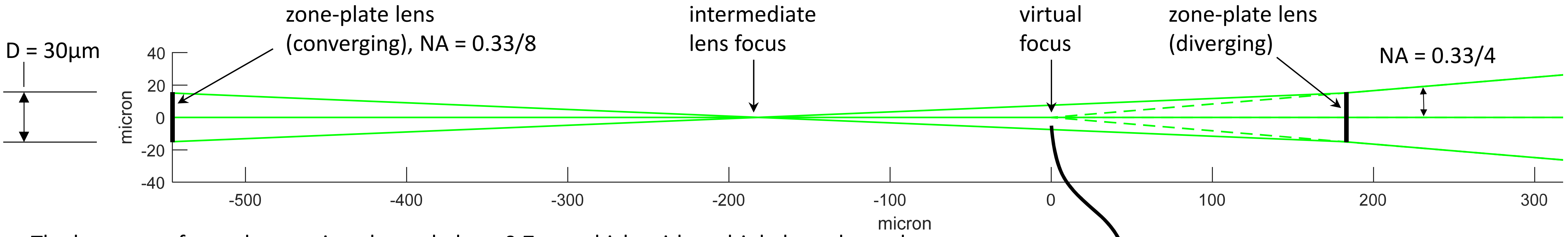

The lenses are formed on a microchannel plate, 0.7-mm thick, with multiple lens channels.
The two lenses can form aberration-free virtual foci at two wavelengths, e.g. 13.365 nm and 13.635 nm.

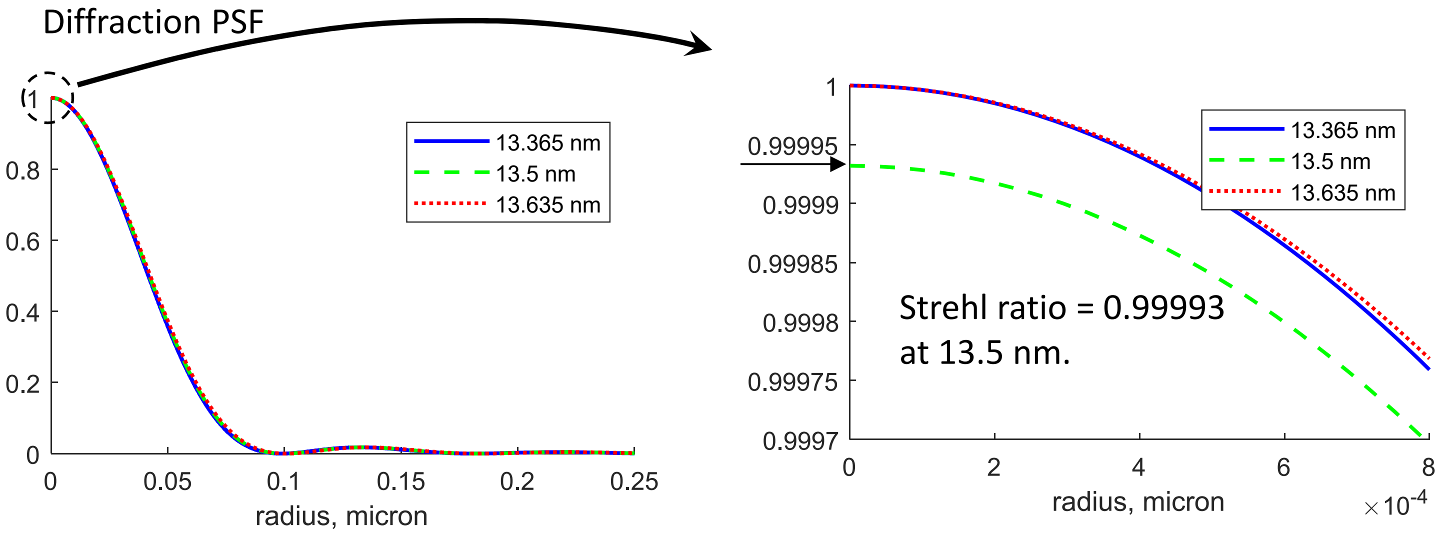

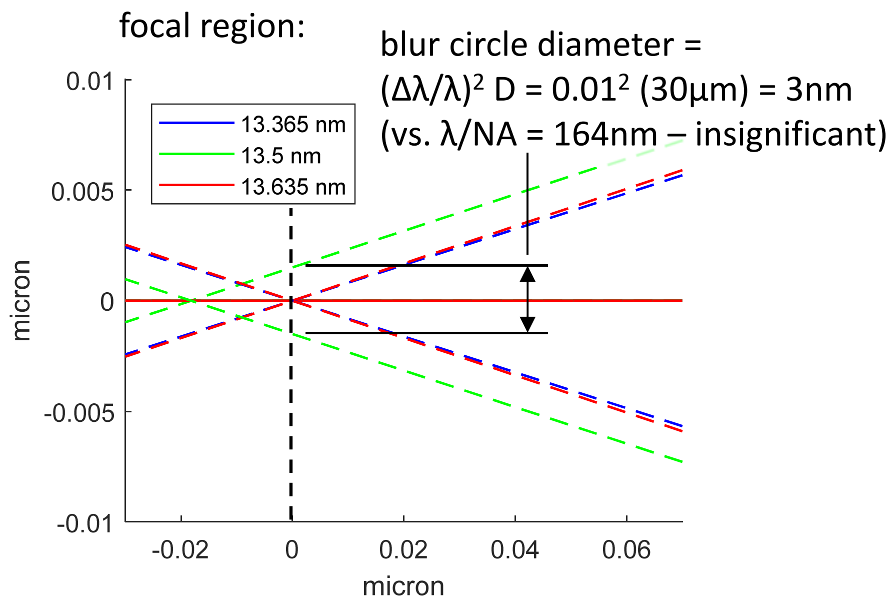

Phase-Fresnel lenses would be ideal for high efficiency.

lens profile for Schupmann doublet, converging element (D = 30µm, NA = 0.33/8, Mo structure on Si membrane):

diverging element:

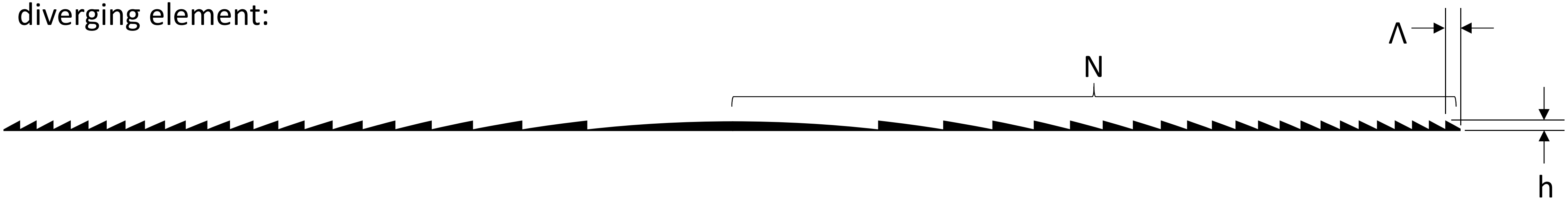

number of zones: $N \approx \frac{1}{4} D\, NA/\lambda = 23$

minimum zone width: $\Lambda = \lambda/NA = 0.327\mu m$

facet height: $h \approx 0.15\mu m$

An ideal sawtooth lens profile can be approximated by a manufacturable stepped profile.

fabrication design concept:

- 3 phase-shift steps, mostly Mo, on 20-nm Si substrate
- Ru etch-stop layers (2 nm)
- Si barrier layers to suppress Mo crystallization (0.2 nm)

EM simulation of comparable line grating:

48% efficiency in 1st transmitted order over full 2% wavelength band (not including fill-factor losses).

For 2-element Schupmann doublet: 23%

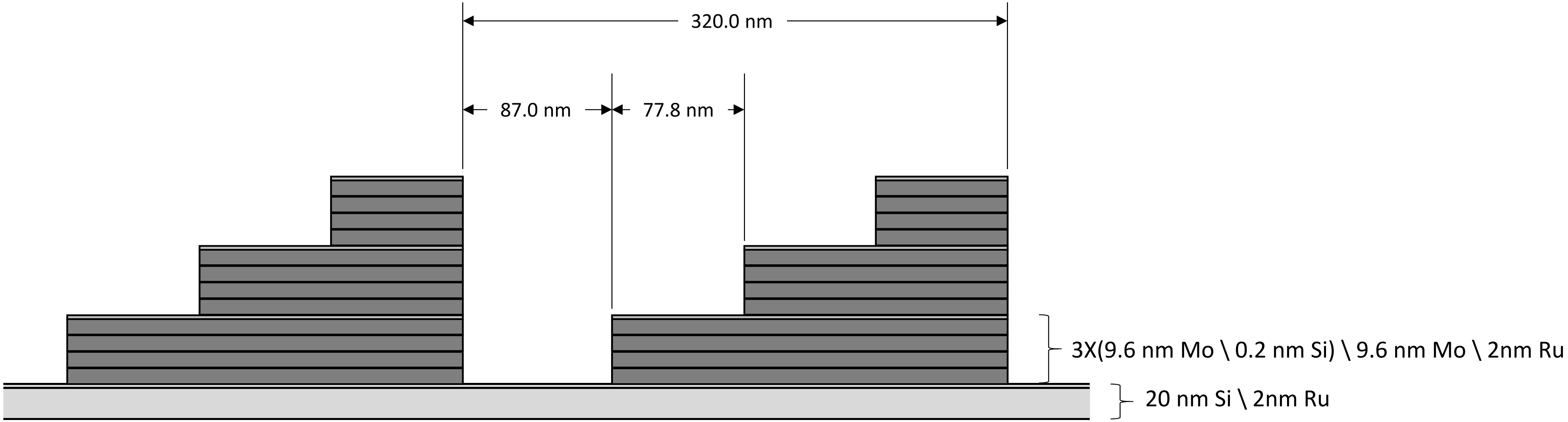

Presentation Outline

1. EUV microlenses can be fully achromatized over a 2% EUV spectrum.

   ✓ **Schupmann-doublet microlenses can provide fully achromatic, aberration-free point imaging with 23% efficiency.**

2. Zero-aberration imaging can be achieved over a large image field with an ***economical*** projection system.

3. A parallel spot-scanning system could provide useful capabilities and benefits for actinic EUV inspection and metrology.

All optical aberrations can be eliminated in the microlens design.

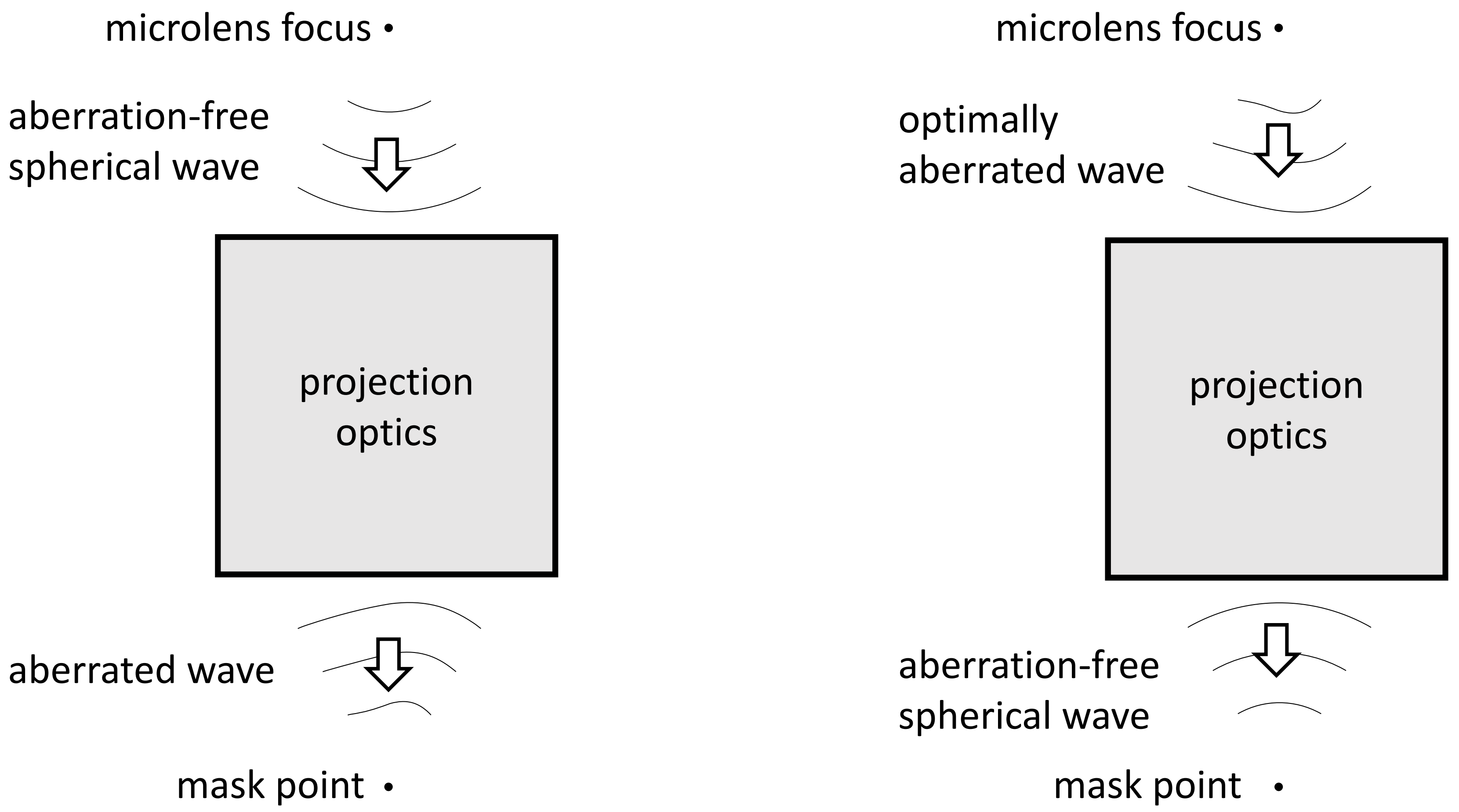

- Each microlens is designed to create an aberration-free point image of the plasma on the mask (compensating for projection optics aberrations).
- The two Schupmann elements can achieve the zero-aberration condition at two wavelengths (sufficient for full achromatization over a 2% band).
- The microlens design can also eliminate any image distortion or field curvature at the mask plane.

The projection system will self-image a 150-mm-radius ring field.

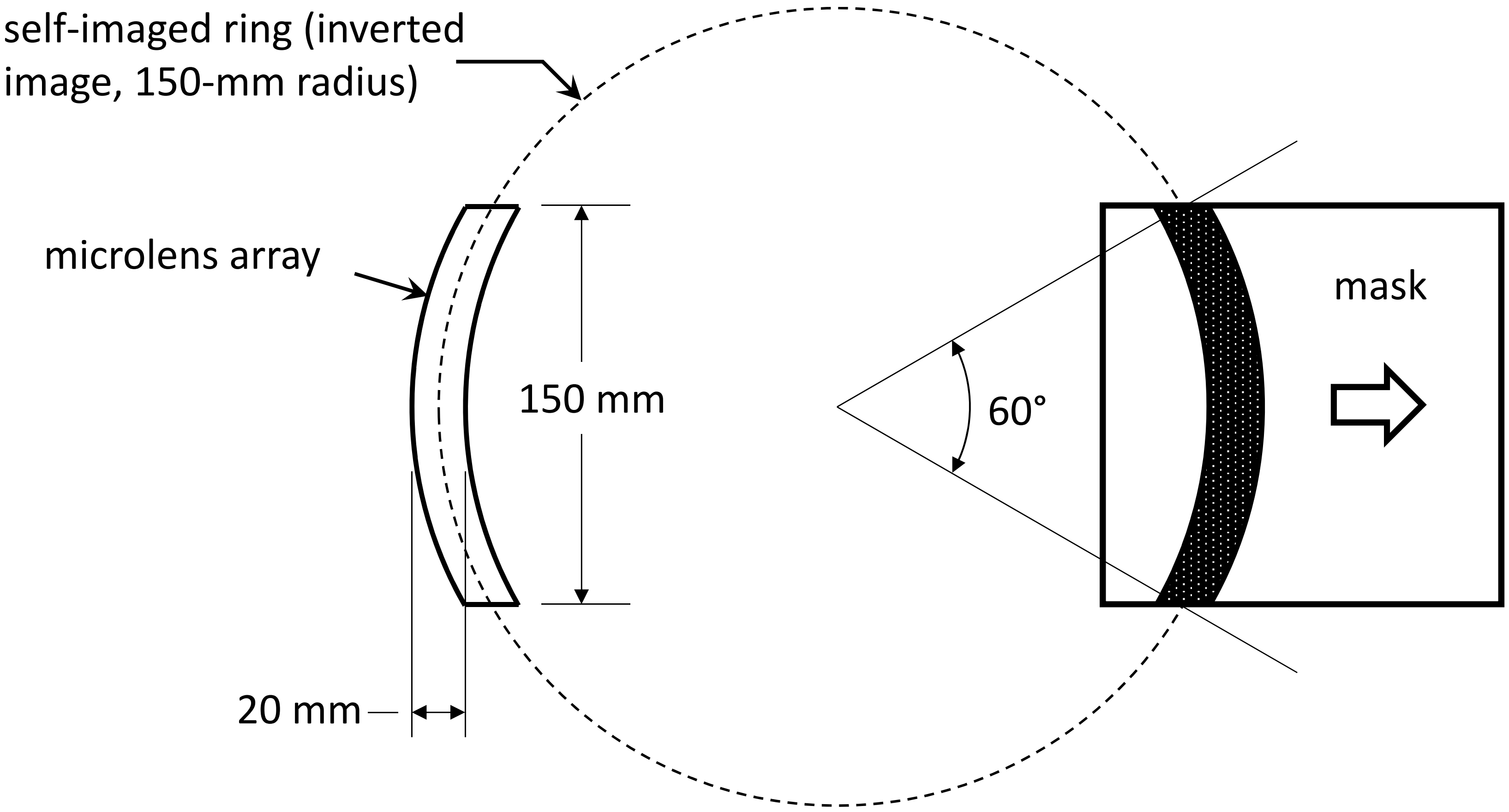

The projection system has good imaging performance on the 150-mm radius, but will require aberration compensation over the full 20-mm field width.

An Offner Projection system consists of two spherical mirrors.

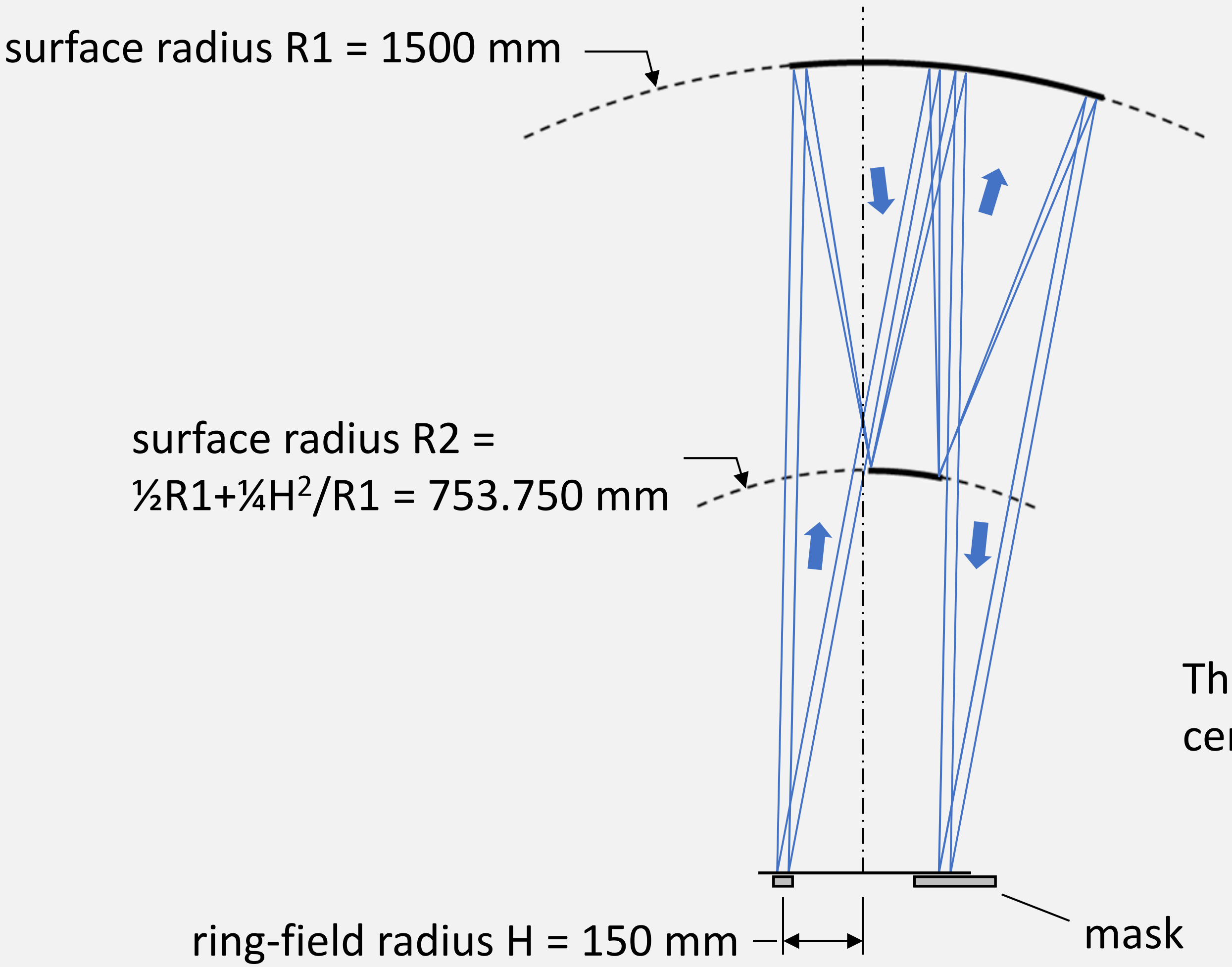

The mirrors are concentric and centered at the middle of the ring field.

The same type of projection system is used on the image collection side.

The illumination and image collection systems are coaxial and share the same ring field.

A fold mirror is used to separate the two projection systems.

Coaxial source collection optics provide illumination to the microlens array.

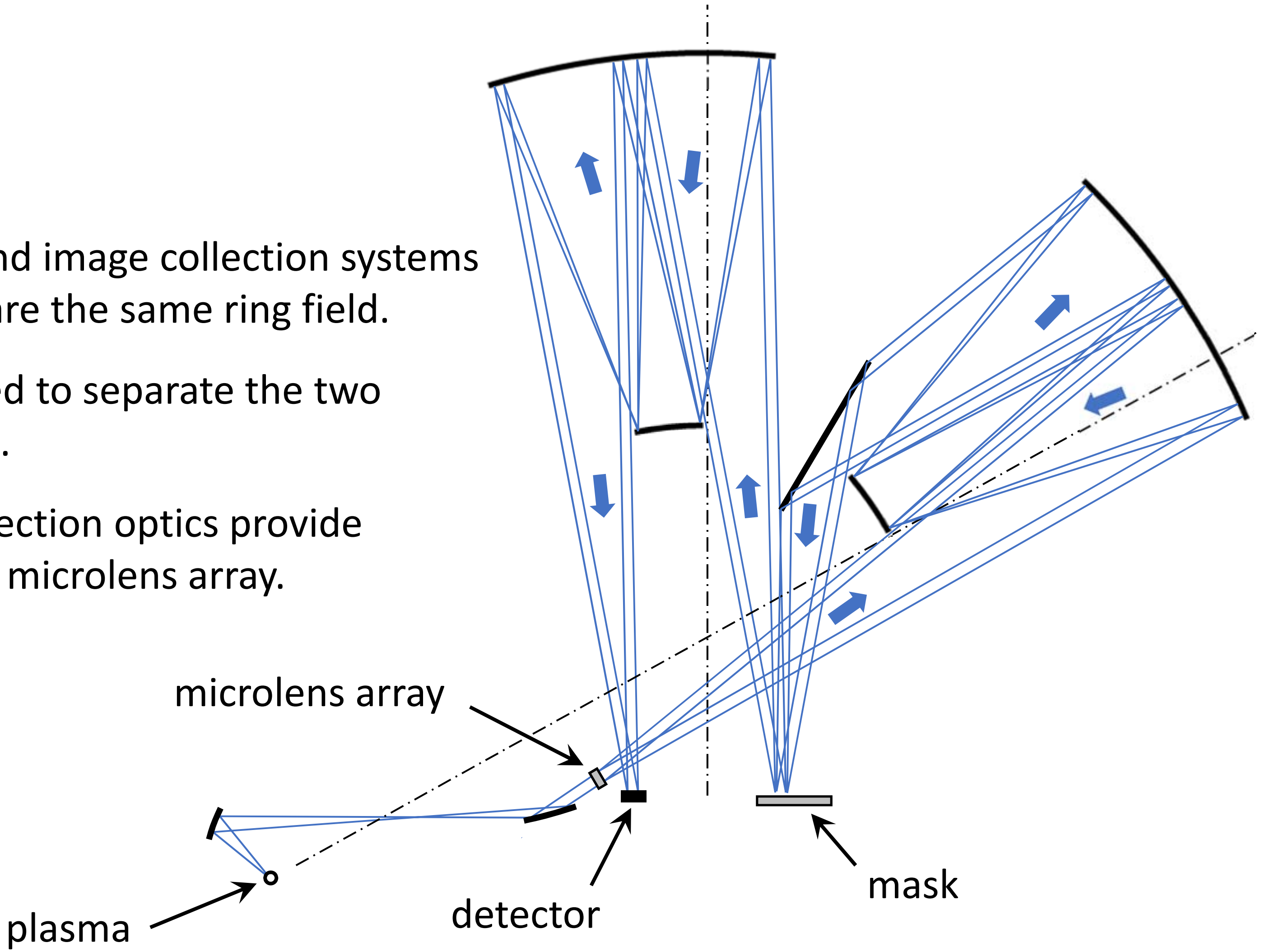

The projection system has about 10 waves (peak-to-valley) astigmatism.

Pupil phase map (wave cycles):

at inner ring radius:
10.5 waves P-V

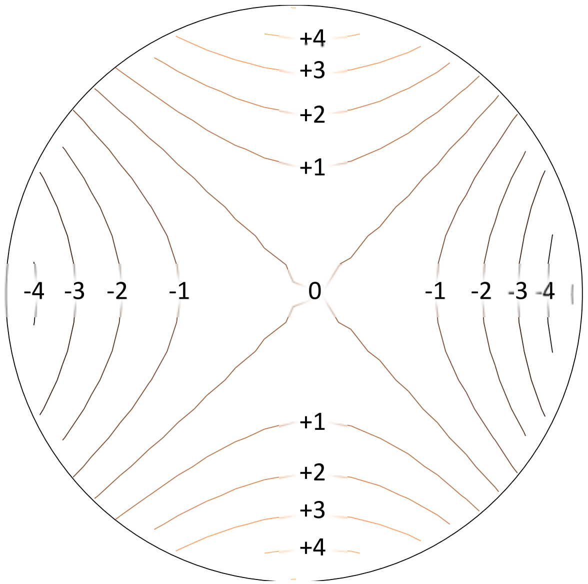

at outer ring radius:
9.6 waves P-V

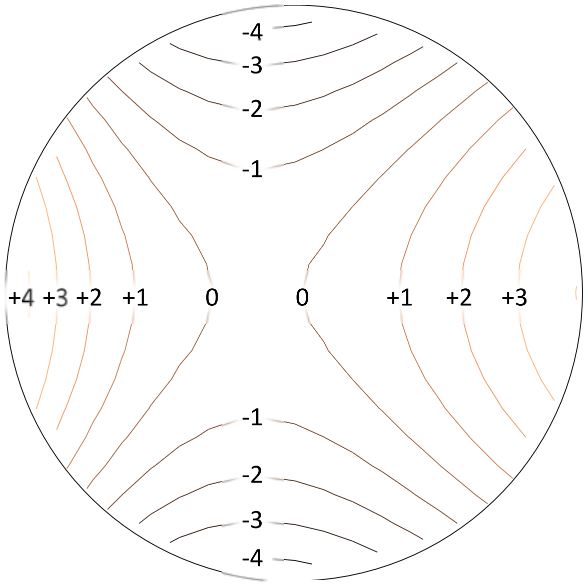

10 waves P-V correction required; each Schupmann element will provide about 5 waves correction.

Astigmatism is corrected by making the microlens phase zones slightly elliptical.

microlens zone pattern, point-focus:

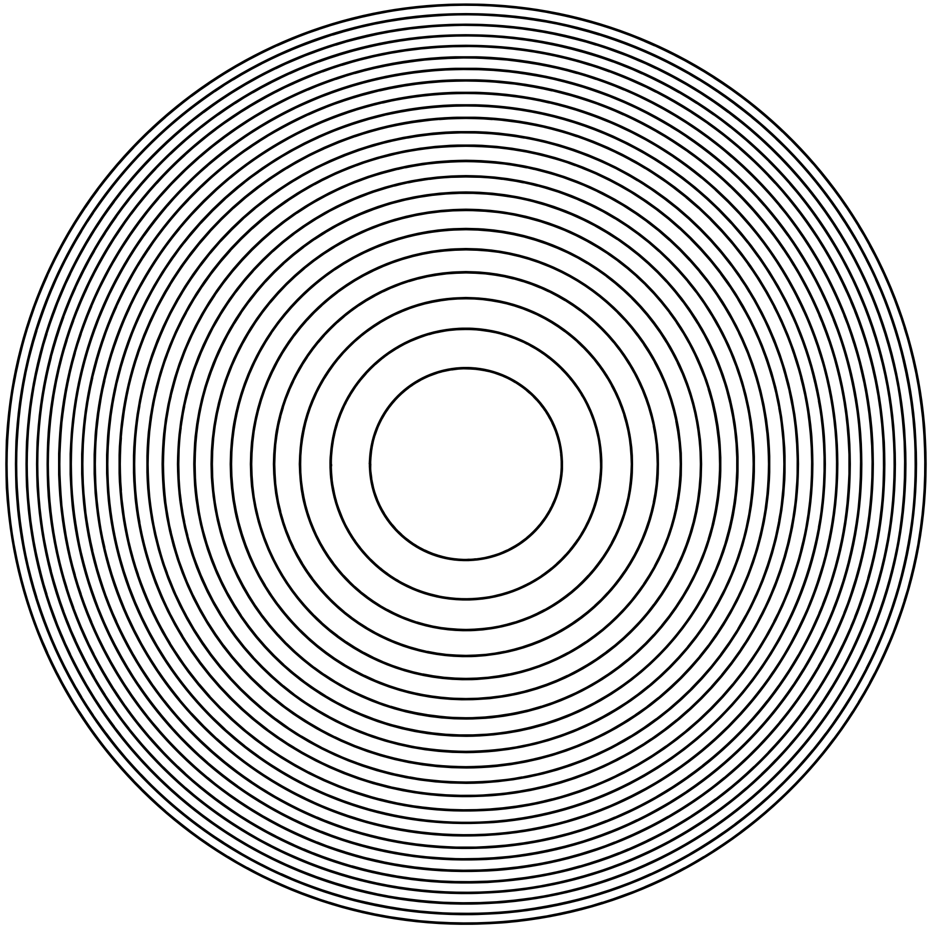

with aberration correction (5 waves P-V):

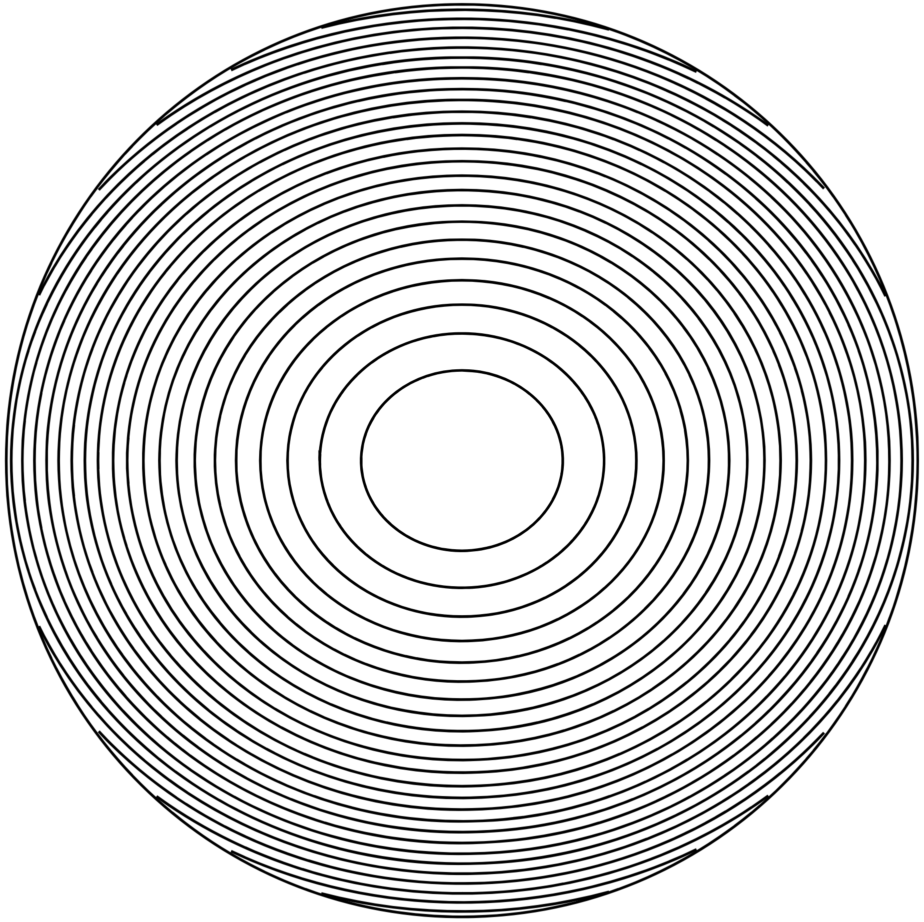

Presentation Outline

1. EUV microlenses can be fully achromatized over a 2% EUV spectrum.

   ✓ **Schupmann-doublet microlenses can provide fully achromatic, aberration-free point imaging with 23% efficiency.**

2. Zero-aberration imaging can be achieved over a large image field with an ***economical*** projection system.

   ✓ **The microlenses can zero out all optical aberrations in the projection system.**

3. A parallel spot-scanning system could provide useful capabilities and benefits for actinic EUV inspection and metrology.

The expansive, mostly empty image field allows access to the far field.

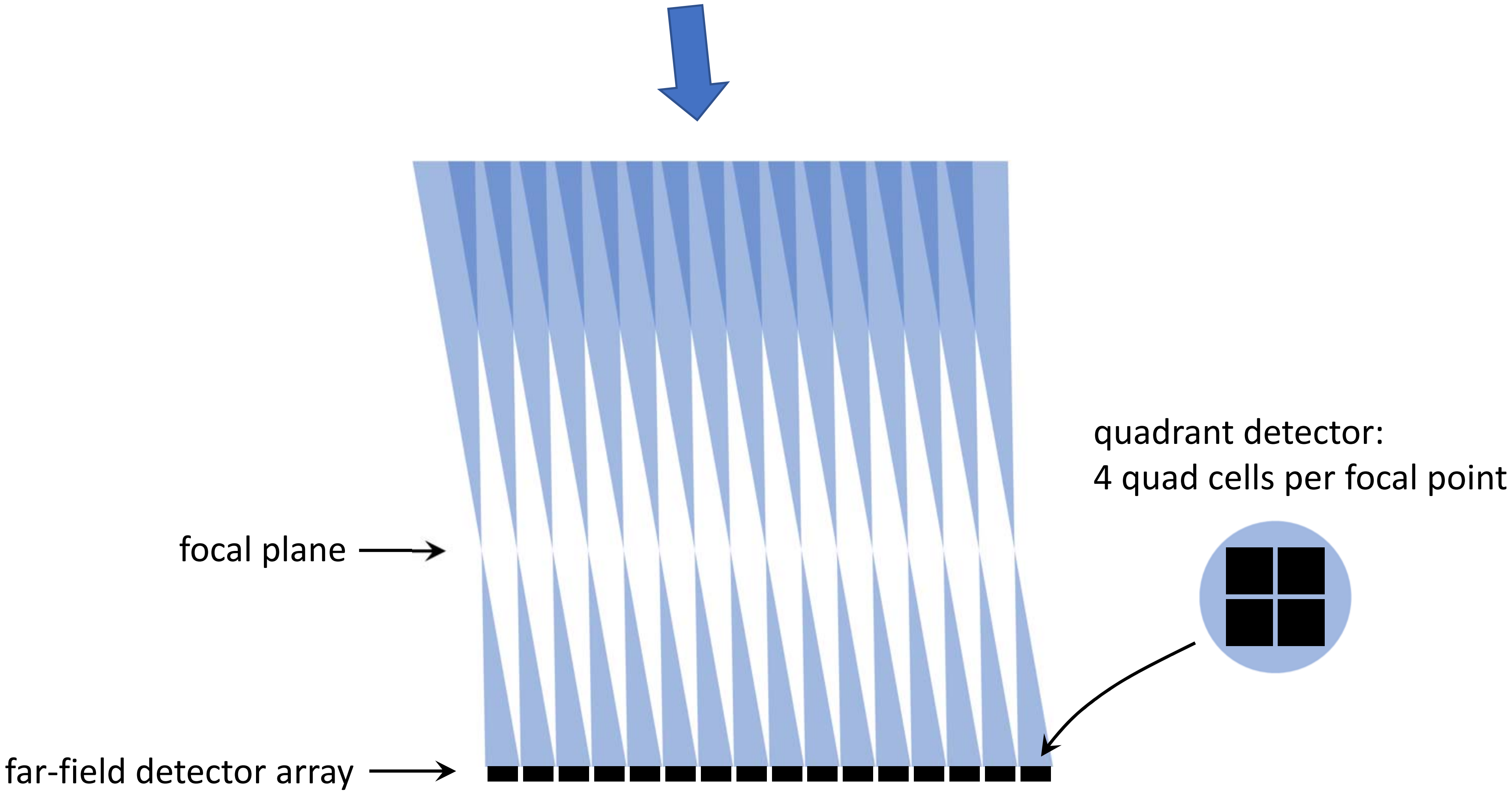

Far-field detection is sensitive to phase defects.

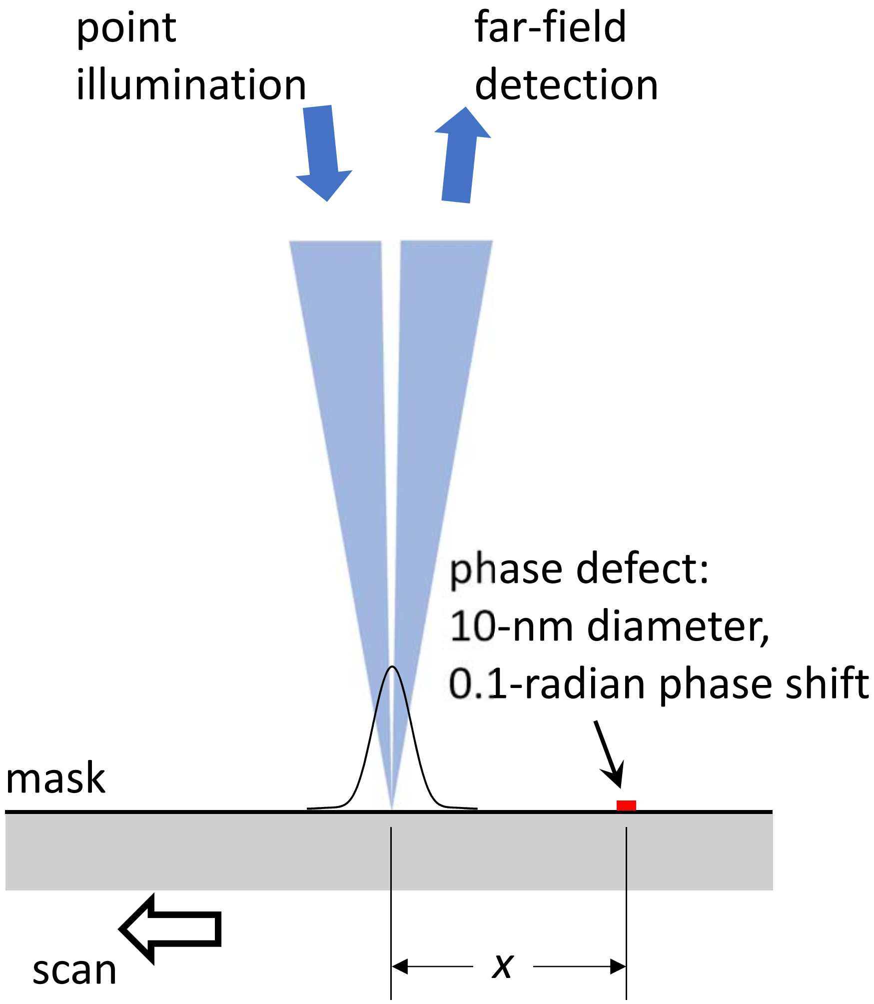

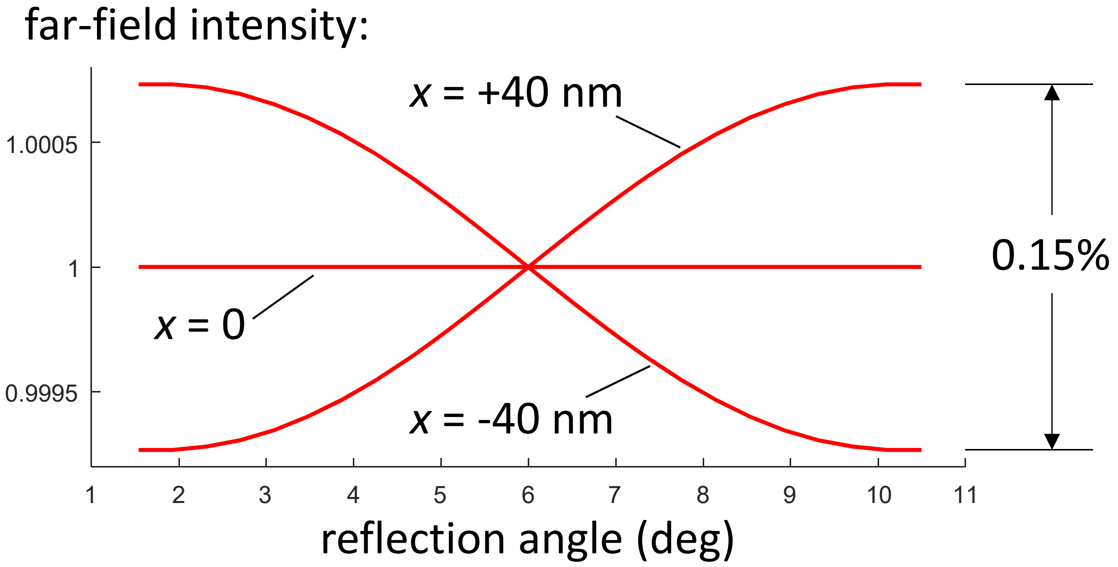

The total (angle-integrated) reflected intensity doesn't change. The defect is only detectable in the intensity distribution over the far field.

The 0.15% intensity asymmetry would be nearly doubled if the plasma were an ideal point source. (A plasma geometric image diameter of 90 nm is assumed in the simulation.) The plasma energy must be spread over many microlenses to achieve sufficient image coherence.

About 2 million microlenses are needed for diffraction-limited focusing.

<u>focus spots:</u>

convergence solid angle
$\Omega = \pi\ NA^2$

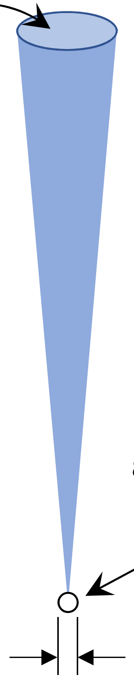

geometric etendu per lens:
$G_{lens} = \Omega\ A < (\frac{1}{2}\ \pi\ \lambda)^2$
$= 4.5 \cdot 10^{-10}\ mm^2 \cdot sr$

geometric image of plasma source

dia. < λ/NA (**diffraction-limited**),
area: $A < \frac{1}{4}\pi(\lambda/NA)^2$

<u>LPP source (Adlyte spec's):</u>

plasma dia. = 60µm,
projected disk area, $A = 0.0028\ mm^2$

plasma

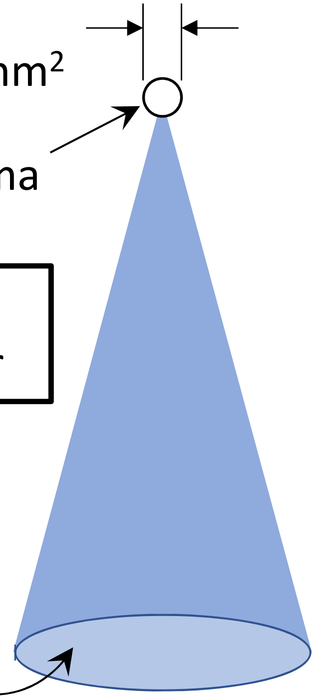

source etendu:
$G_{source} = \Omega\ A = 5.7 \cdot 10^{-4}\ mm^2 \cdot sr$

collection solid angle:
$\Omega = 0.2sr$

Minimum number of lenses:
$N_{lens} \approx G_{source} / G_{lens} > 1.3 \cdot 10^6$ (minimum)

We will use $N_{lens} = 2 \cdot 10^6$.

The etendu captured by each lens will be limited by the lens fill factor η_{FF}: $G_{lens} = (G_{source} / N_{lens})\ \eta_{FF}$.

The lens center spacing is about 40 µm and the raster line spacing is about 80 nm.

ring field:

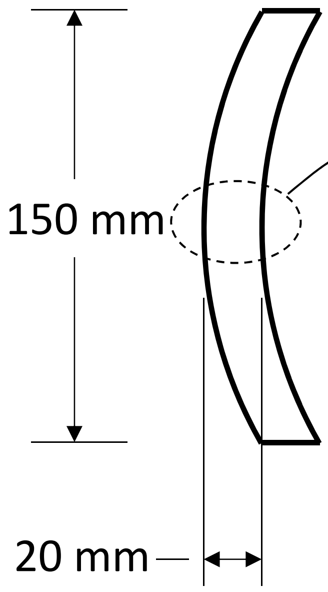

microlens rows & raster lines:

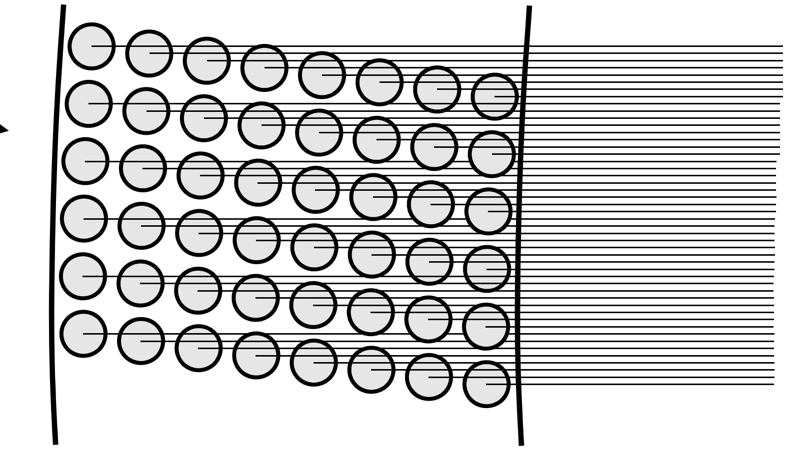

field area per microlens with $N_{lens} = 2 \cdot 10^6$:

$A_{lens} = (150\text{ mm})\cdot(20\text{ mm})/(2\cdot 10^6) = 0.0015\text{ mm}^2$

Assume square-grid lens centering (although hexagonal would be more efficient). Lens center spacing is $\sqrt{A_{lens}} = 38.7\mu m$.

microlens diameter D = 30µm

lens fill factor $\eta_{FF} = \pi\,(D/2)^2/\,A_{lens} = 0.47$

lenses per row:

$N_{lens/row} \approx (20\text{ mm})/(38.7\mu m) \approx 516$

raster line spacing (single-pass):

$\delta_{line} \geq (38.7\mu m)/516 = 75\text{ nm}$

(We will use 80 nm. Multiple scan passes are required for a denser scan.)

The detector signal is about 700 photons per quad cell per laser pulse.

source radiance at IF within 2% λ band (Adlyte): L_{IF} = 1000 W/mm²·sr

in-band EUV power at IF: $\Phi_{IF} = L_{IF}\, G_{source}$ = 0.57 W

estimated system transmittance, IF to detector: $\eta = (0.68)^9 \cdot 0.23 \cdot 0.47 = 0.0034$
- 6 near-normal-incidence mirror reflections (approx. 68%)
- 2 grazing-incidence reflections (approx. 68%)
- mask (approx. 68%)
- Schupmann doublet efficiency (23%)
- lens fill factor (47%)

number of quad cells (4 per lens): $N_{quad\text{-}cell} = N_{lens} \cdot 4 = 8 \cdot 10^6$

collected power per quad cell: $\Phi_{quad\text{-}cell} = \eta\, \Phi_{IF} / N_{quad\text{-}cell} = 2.4 \cdot 10^{-10}$ W

laser rep rate (Adlyte spec): $2.3 \cdot 10^4\ \text{sec}^{-1}$

energy per quad cell per laser pulse: $Q_{quad\text{-}cell} = \Phi_{quad\text{-}cell} / \nu = 1.0 \cdot 10^{-14}$ J

EUV photons per quad cell per laser pulse: $Q_{quad\text{-}cell} \cdot (6.242 \cdot 10^{18}$ eV/J)/(92 eV/photon) = 700 photons

Use 4-pulse binning (4 pulses per image frame) to get 2800 photons per quad cell per frame (11200 photons per focus point per frame).

Throughput is < 2hrs scan time per mask.

The sampling grid step should be << $\lambda/(2\ NA) = 82nm$

Set the scan grid step to $\delta_X = 5nm$ per laser pulse (20nm per image frame @ 4 pulses per frame).

Set the cross-scan grid step to $\delta_Y = 20nm$. (Do 4 scan passes with 80-nm raster line spacing.)

total scan area: $A_{scan} = (150\ mm)\cdot(190\ mm)$

total number of grid points: $N_{grid} = A_{scan}/(\delta_X \cdot \delta_Y) = 2.9\cdot 10^{14}$

number of laser pulses: $N_{pulse} = N_{grid} / N_{lens} = 1.4\cdot 10^{8}$

pulses per sec: $\nu = 2.3\cdot 10^{4}\ sec^{-1}$

scan time: $t_{scan} = N_{pulse} / \nu = 6.2\cdot 10^{3}$ sec = 103 min per scan

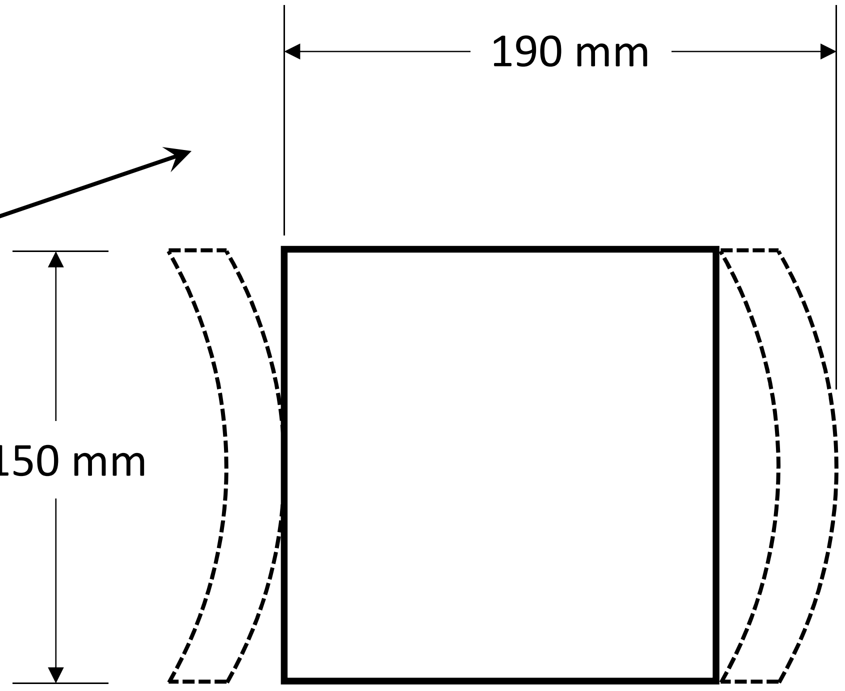

Conclusions

1. EUV microlenses can be fully achromatized over a 2% EUV spectrum.

   ✓ **Schupmann-doublet microlenses can provide fully achromatic, aberration-free point imaging with 23% efficiency.**

2. Zero-aberration imaging can be achieved over a large image field with an ***economical*** projection system.

   ✓ **The microlenses can zero out all optical aberrations in the projection system.**

3. A parallel spot-scanning system could provide useful capabilities and benefits for actinic EUV inspection and metrology.

   ✓ **zero-aberration, diffraction-limited illumination points for high detection sensitivity**

   ✓ **far-field detection for good phase sensitivity**

   ✓ **full-mask scan with high throughput**

Selected References

EUV microscopes:

K. A. Goldberg et al., "Commissioning an EUV mask microscope for lithography generations reaching 8 nm", Proc. SPIE 8679, Extreme Ultraviolet (EUV) Lithography IV, 867919 (1 April 2013)
https://doi.org/10.1117/12.2011688
https://cloudfront.escholarship.org/dist/prd/content/qt9zw2b2w1/qt9zw2b2w1.pdf

P. P. Naulleau et al., "Electro-optical system for scanning microscopy of extreme ultraviolet masks with a high harmonic generation source," Opt. Express 22, 20144-20154 (2014)
https://doi.org/10.1364/OE.22.020144

K. C. Johnson, US Patent App. 15/269,848, 2017

K. Johnson, "Zero-Aberration, Actinic, EUV Mask Inspection Microscope with High Defect Sensitivity", 2016
http://vixra.org/pdf/1511.0139v2.pdf

Diffractive Schupmann lenses:

K. Johnson, "Scanned-spot-array extreme ultraviolet imaging for high-volume maskless lithography", Journal of Vacuum Science & Technology B, Nanotechnology and Microelectronics: Materials, Processing, Measurement, and Phenomena 30, 051606 (2012)
https://doi.org/10.1116/1.4752112

EUV zone plate fabrication:

F. H. Salmassi et al., "Fabrication and performance of transmission engineered molybdenum-rich phase structures in the EUV regime (Conference Presentation)", Proc. SPIE 10450, International Conference on Extreme Ultraviolet Lithography 2017, 104501B (16 October 2017)
https://doi.org/10.1117/12.2281487

Projection system:

A. Offner, U.S. Patent 3,748,015 (1973).

Adlyte LPP source:

R. S. Abhari et al., "Laser-produced plasma light source for extreme-ultraviolet lithography applications," Journal of Micro/Nanolithography, MEMS, and MOEMS 11(2), 021114 (11 June 2012).
https://doi.org/10.1117/1.JMM.11.2.021114
https://www.researchgate.net/profile/Oran_Morris/publication/244994879_Laser-produced_plasma_light_source_for_extreme-ultraviolet_lithography_applications/links/590986920f7e9b1d08147991/Laser-produced-plasma-light-source-for-extreme-ultraviolet-lithography-applications.pdf
http://www.adlyte.com/

EUV detectors:

D. T. Wintz et al., "Photon flux requirements for EUV reticle imaging microscopy in the 22- and 16nm nodes", Proc. SPIE 7636, Extreme Ultraviolet (EUV) Lithography, 76362L (22 March 2010)
https://doi.org/10.1117/12.846528
https://www.osti.gov/scitech/servlets/purl/983198